

## Resistivity of Iron as a Function of Temperature and Magnetization\*

G. R. TAYLOR, ACAR ISIN, AND R. V. COLEMAN

*Department of Physics, University of Virginia, Charlottesville, Virginia*

(Received 28 July 1967)

The temperature dependence of the resistance of iron has been measured in the range 1 to 4.2°K. Single-crystal iron specimens 100 to 300  $\mu$  in diameter with residual resistance ratios up to 2100 were used in the experiments. The dominant temperature dependence in this range is linear with average coefficients of  $8.2 \times 10^{-4}$  and  $2.14 \times 10^{-4} \mu_A \text{ cm}/^\circ\text{K}$  in the flux-closed and -saturated states, respectively. These coefficients are an order of magnitude larger than those observed by previous experimenters. Careful control of the magnetic state of the crystal seems to remove most of the  $T^2$  dependence in this temperature range. The results are discussed in terms of the general electron-magnon scattering theories developed by Turov. Deviations from Ohm's law and large negative magnetoresistance effects are observed, and these are taken into account in making the measurements. Preliminary measurements have also been made in the range 77 to 294°K, and results are in general agreement with previous measurements by White and Woods.

### INTRODUCTION

WE have measured the temperature dependence of resistance for iron in the range 1 to 4.2°K. The specimens were iron whiskers 100–300  $\mu$  in diameter and up to 2 cm long. From sample characterization data reported in the following sections, we conclude that these samples are up to an order of magnitude more pure than samples used in previous measurements of this type. The major contribution to the temperature-dependent resistivity in the 1 to 4.2°K range is expected to be magnon-electron scattering. We find a dominant linear dependence of resistivity on temperature and have measured the appropriate coefficients for both  $\langle 100 \rangle$  and  $\langle 111 \rangle$  axial whiskers. These results are compared to the spin-wave scattering theories of Turov<sup>1–3</sup> and Vonsovski.<sup>4</sup>

To first approximation we find no dependence of the coefficient on crystal orientation. Measurements have been made for both the flux-closed multidomain state and for the approximately single-domain state attained by saturating the crystal in a longitudinal field of 1000 Oe. The linear coefficients for these two magnetic states differ by a factor of 3.8 with  $\alpha_{FC} = 3.8 \times \alpha_{PS}$ . Within experimental error, the data show only a linear temperature dependence for both the flux closed and partially saturated states. Any  $T^2$  coefficient is extremely small and within limits discussed in the section on discussion of experimental results.

The iron specimens used in the experiments show a large negative magnetoresistance which can represent up to a 90% reduction in the resistance of the specimen. In addition, a large deviation from Ohm's law behavior is observed particularly in the flux-closed multidomain state. Both of these effects have important consequences

to the measurement of the temperature coefficient and these are discussed in the following sections.

We have also compared our results to previous data, particularly that of Semenenko and Sudovtsov.<sup>5,6</sup> In general, our linear coefficient appears to be an order of magnitude larger than that found in previous measurements while any  $T^2$  component is appreciably smaller. We attribute these results to the higher purity of our specimens and to a better control of domain structure effects.

### MAGNETORESISTANCE

The field dependence of the longitudinal magnetoresistance of iron whiskers at 4.2° is shown in Fig. 1, along with the magnetization curves for bulk single crystals of the same orientation. The magnetoresistance is strongly negative and the shape of the curve follows closely the expected magnetization curves. The initial sharp drop in resistance for both  $\langle 100 \rangle$  and  $\langle 111 \rangle$  orientations occurs during magnetization by domain boundary motion while in the  $\langle 111 \rangle$  a second region of lower slope occurs which can be identified with magnetization by coherent spin rotation in higher fields. The initial sharp drop in resistance shows a substantial hysteresis when the field is cycled and therefore indicates a strong connection between magnetization by domain wall motion and the initial negative magnetoresistance. Figure 2 shows typical hysteresis curves obtained for  $\langle 100 \rangle$  and  $\langle 111 \rangle$  iron whiskers. The maximum in resistance always occurs at the flux-closed or  $M=0$  state designated by FC while a minimum in resistance occurs when the specimen is largely saturated in fields of several hundred Oe. This is designated as the partially saturated state PS. The initial zero-field domain structure of the specimens is shown in Fig. 3

\* Research supported in part by the U.S. Atomic Energy Commission and the Army Research Office, Durham.

<sup>1</sup> E. A. Turov, *Izv. Akad. Nauk. USSR Ser. Fiz.* **19**, 462 (1955).

<sup>2</sup> E. A. Turov, *Izv. Akad. Nauk. USSR Ser. Fiz.* **19**, 474 (1955).

<sup>3</sup> E. A. Turov, *Fiz. Metal. Metalloved.* **6**, 203 (1958).

<sup>4</sup> S. V. Vonsovski, *Izv. Akad. Nauk. USSR Ser. Fiz.* **19**, 447 (1955).

<sup>5</sup> A. I. Sudovtsov and E. E. Semenenko, *Zh. Eksperim. i Teor. Fiz.* **31**, 525 (1956) [English transl.: *Soviet Phys.—JETP* **4**, 592 (1957)].

<sup>6</sup> E. E. Semenenko and A. I. Sudovtsov, *Zh. Eksperim. i Teor. Fiz.* **42**, 1022 (1962) [English transl.: *Soviet Phys.—JETP* **15**, 708 (1962)].

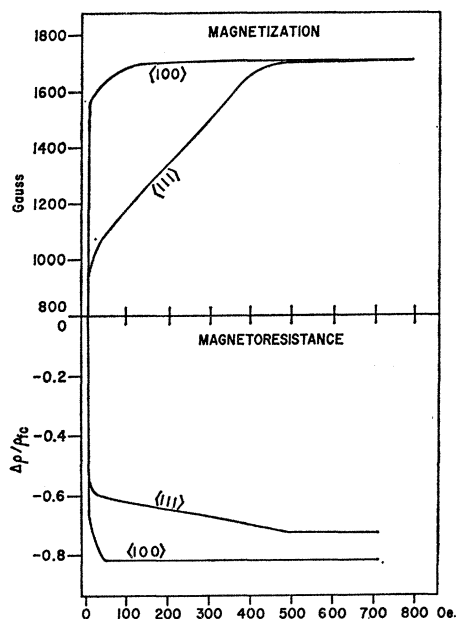


FIG. 1. Field dependence of the longitudinal magnetoresistance of iron whiskers, lower curves. Magnetization curves for bulk single crystals, upper curves.

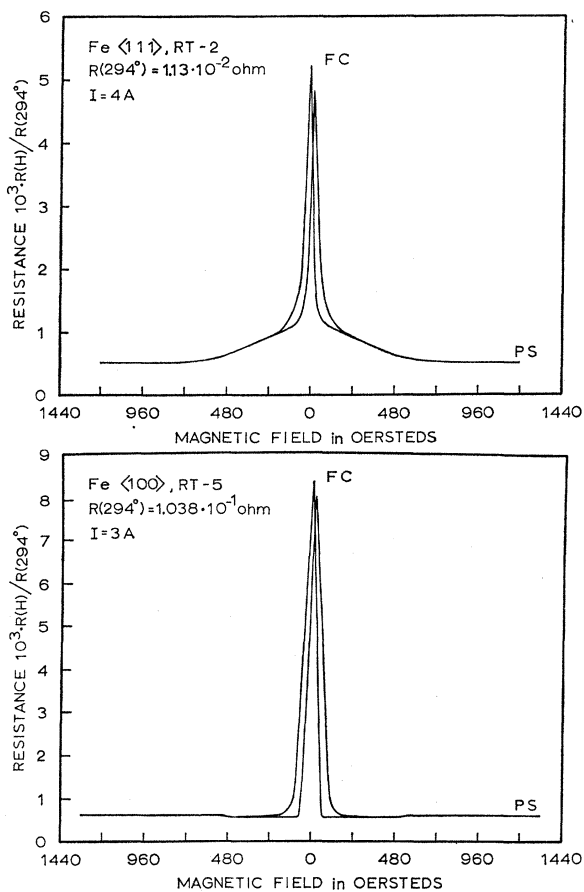


FIG. 2. Magnetoresistance hysteresis curves obtained for  $\langle 100 \rangle$  and  $\langle 111 \rangle$  iron whiskers.

and has been established by extensive work with powder patterns.<sup>7-9</sup>

The source of the negative magnetoresistance behavior is not completely certain at this time. Several mechanisms could contribute to the large extra resistance observed in the flux closed state as compared to the single-domain state. These include domain boundary scattering, reverse galvanomagnetic effect, size effects related to the presence of domain boundaries, and changes in the spin-wave spectrum due to domain boundaries. The observed negative magnetoresistance is, however, a very sensitive function of the measuring current and any explanation must take account of the strong deviations from Ohm's law observed in the flux-closed state. The large negative magnetoresistance in iron whiskers has been observed and discussed by a number of authors, including Isin and Coleman,<sup>10,11</sup> Reed, and Fawcett,<sup>12</sup> and Dheer.<sup>13</sup>

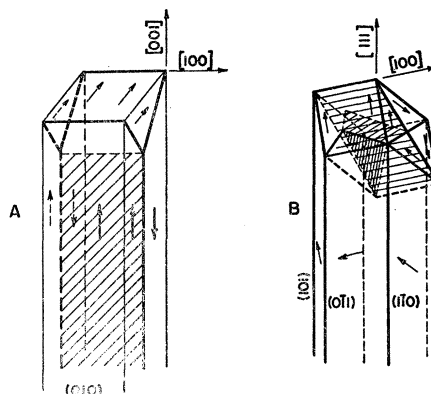


FIG. 3. Zero-field domain structure of  $\langle 100 \rangle$  and  $\langle 111 \rangle$  iron whiskers deduced from powder pattern observations.

### DEVIATIONS FROM OHM'S LAW

The detailed shape of the low-field magnetoresistance curves shows a critical dependence on the measuring current. This is particularly true for currents below 1 amp. The best way of showing this effect is to plot the resistance at a given point on the magnetoresistance curve as a function of measuring current. Such a plot for a  $\langle 100 \rangle$  axial specimen is shown in Fig. 4, and includes the resistance at the flux-closed (FC) and partially saturated (PS) state of the magnetoresistance curve. Plots for temperatures of 4.2 and 1°K are shown. The resistance values in these plots are normalized to the measured room temperature resistance which agrees

<sup>7</sup> R. V. Coleman and G. G. Scott, Phys. Rev. **107**, 1276 (1957).  
<sup>8</sup> R. V. Coleman and G. G. Scott, J. Appl. Phys. **29**, 526 (1958).  
<sup>9</sup> R. W. DeBlois and C. D. Graham, J. Appl. Phys. **29**, 931 (1958).

<sup>10</sup> A. Isin and R. V. Coleman, Phys. Rev. **142**, 372 (1966).

<sup>11</sup> R. V. Coleman and A. Isin, J. Appl. Phys. **37**, 1028 (1966).

<sup>12</sup> W. A. Reed and E. Fawcett, Phys. Rev. **136**, A422 (1964).

<sup>13</sup> P. N. Dheer, Phys. Rev. **156**, 637 (1967).

with the published values of the resistivity of bulk iron at room temperature.

It is clear from the plot that the FC magnetic state shows a strong deviation from Ohm's law while the PS state follows Ohm's law rather closely. At high currents ( $> 1$  amp) the flux closed resistance approaches an Ohm's law behavior. The data from these plots also indicate that for the  $\langle 100 \rangle$  axial whiskers the observed negative magnetoresistance is almost entirely due to the rise of resistance in the FC state induced by the measuring current. These observations suggest that for the  $\langle 100 \rangle$  axial whiskers a reverse galvanomagnetic effect as schematically pictured in Fig. 5 may be responsible for the negative longitudinal magnetoresistance in  $\langle 100 \rangle$  specimens. The figure indicates the sequence of spin orientations relative to the crystal axis that can occur as first current and then magnetic field is applied parallel to the crystal axis. Figure 5(a) shows the zero current, zero field state determined by powder patterns. The spin configuration shown in Fig. 5(b) is favorably oriented with respect to the self-field of the current and can be obtained using only  $\langle 100 \rangle$  easy directions and developing no demagnetizing effects. Application of an external longitudinal field would again orient all spins parallel to the axis, leaving only a cap structure at the end of the crystal due to demagnetizing effects, Figure 5(c). The negative magnetoresistance and deviations from Ohm's law can then

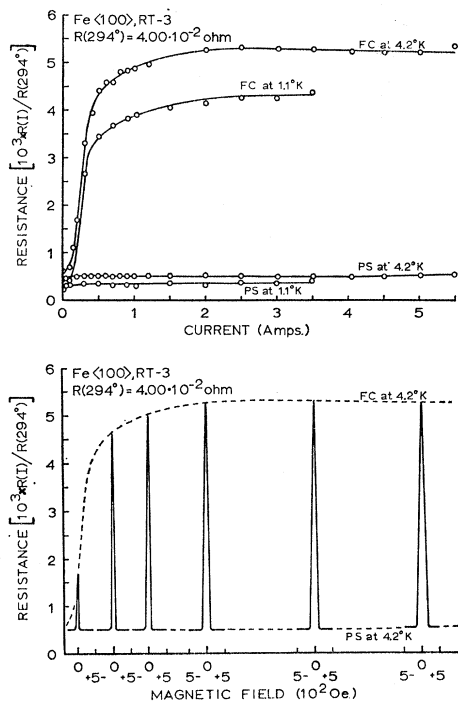


FIG. 4. Resistance as a function of measuring current for the flux closed and partially saturated state of a  $\langle 100 \rangle$  iron whisker. Curves for 4.2 and 1.1°K are shown. Lower curve shows observed negative magnetoresistance as a function of measuring current.

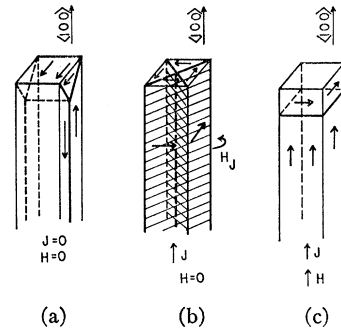


FIG. 5. Diagram showing a sequence of possible domain configurations resulting from applied currents and magnetic fields. (a) Zero-current, zero-field state. (b) domain structure resulting from self-field of the current, (c) final partially saturated domain configuration.

be explained by observing that the magnetoresistance of domains with  $\mathbf{M} \perp \mathbf{J}$  is much higher than the magnetoresistance of domains with  $\mathbf{M} \parallel \mathbf{J}$ . In the case of  $\langle 100 \rangle$  axial specimens this interpretation seems to account for all of the observations. The reverse galvanomagnetic effect has also been used by Tatsumoto<sup>14</sup> and by Berger and deVroomen<sup>15</sup> to explain similar observations in iron.

In the case of the  $\langle 111 \rangle$  axial whisker, however, such a simple interpretation does not give a complete picture. The resistance as a function of measuring current is shown in Fig. 6 for temperatures of 1 and 4.2°K. We have plotted resistance at the intermediate state before coherent spin rotation begins (SR), and in the nearly saturated state after coherent spin rotation is complete (PS). Both the PS and SR magnetic state follow Ohm's law fairly closely while the FC state resistance again shows a strong deviation. We conclude that the sharp initial region of negative magnetoresistance is again induced by the measuring current while the second region of negative magnetoresistance corresponds to the coherent spin rotation process and is independent of current. A possible sequence of spin orientations is shown in Fig. 7.

In the case of the  $\langle 111 \rangle$  axial crystal the initial spin directions are distributed among the 6  $\langle 100 \rangle$  directions that make angles of either 55° or (180°-55°) to the  $\langle 111 \rangle$  axis. This zero current, zero field configuration is shown in Fig. 7(a) and is already the most favorably oriented one with respect to the self-field of the current that can be obtained using  $\langle 100 \rangle$  easy directions of magnetization. Application of a weak longitudinal field should produce domain boundary motion resulting in a longitudinal magnetization utilizing  $\langle 100 \rangle$  easy directions in a structure similar to that shown in Fig. 7(c). Any of the domain structures utilizing  $\langle 100 \rangle$  spin directions involve domains with  $\mathbf{M}_s$  either at 55° to  $\mathbf{J}$  or at (180°-55°) to  $\mathbf{J}$ , and both should have the

<sup>14</sup> E. Tatsumoto, Phys. Rev. **109**, 658 (1958).

<sup>15</sup> L. Berger and A. R. deVroomen, J. Appl. Phys. **36**, 2777 (1956).

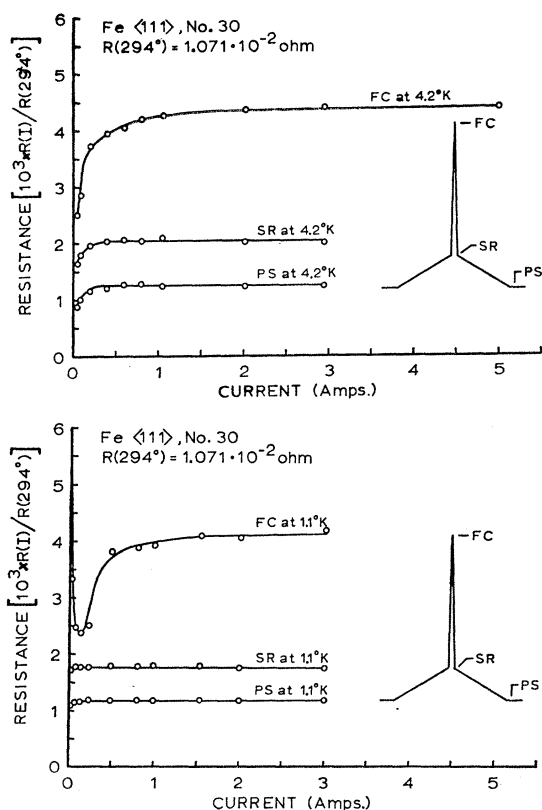


FIG. 6. Resistance as a function of measuring current for  $\langle 111 \rangle$  axial whisker. Curves show resistance at 4.2 and 1.1°K for the flux closed and partially saturated state.

same magnetoresistance, since it is proportional to  $\cos^2\theta$ . Therefore, the initial sharp drop in resistance is not accounted for by reverse galvanomagnetic effects unless the self-field of the current can rotate spins into hard directions which seems unlikely. Such a rotation would orient the spin in a  $\langle 211 \rangle$  direction making an angle of  $90^\circ$  with the current direction. [See Fig. 7(b)]. This direction is still in the (110) plane so that no surface pole development is involved (demagnetizing effect). If the  $\langle 211 \rangle$  anisotropy energy were small this might be a possibility. The resulting domain walls would be  $60^\circ$  walls, however, and this would also involve some extra energy. The added magnetoresistance due to the  $\cos^2\theta$  term would be in approximate agreement with the observed result since  $\cos^2 90^\circ = 1.000$  and  $\cos^2 55^\circ = 0.3290$  giving a ratio  $R_{FC}/R_{SR}$  of 3 which is approximately the one observed at high measuring currents (greater than 1 A).

The above discussion serves to characterize the specimens used in these experiments. Although we are not completely sure of the explanation for the behavior observed, it is clear that any attempt to measure the temperature dependence in the 1 to 4.2°K range should take account of these effects in such a way that they do not introduce spurious changes in resistance as a function of temperature. The next section outlines

the sample characterization of the specimens used in the temperature dependence experiments.

### SAMPLE CHARACTERIZATION

We have measured the temperature dependence of resistance for seven iron specimens varying from 100 to 300  $\mu$  in diameter. The room-temperature resistance for five of the specimens corresponded exactly with the resistivity values published for bulk iron. Two of the  $\langle 100 \rangle$  specimens were calculated to have lower resistivity values at room temperature than bulk, but a probable source of this error is in the measurement of dimensions. The data were analyzed using ratios  $R(T)/R(294^\circ\text{K})$  so that the dimensional dependence was eliminated and comparison of the final data can be made independently of specific sample dimension. Table I lists the relevant data for the seven specimens used. The residual resistance ratios  $R(294^\circ\text{K})/R(4.2^\circ\text{K})$  are given for the two magnetic states at 4.2°K, flux closed (FC) and partially saturated (PS). The ratio for the partially saturated state indicates an upper maximum for any impurity contribution to the resistance and ranges as high as several thousand indicating a very high purity for these samples. The flux closed ratio is of course much lower because of the large additional magnetic resistance at 4.2°K. The table also indicates the magnetoresistance ratio  $\Delta R(H)/R(4.2^\circ\text{K})$  in percent observed for each specimen. The current at which the 4.2°K data was measured is indicated for each specimen in the last column of the table. These were also the measuring currents used for the temperature dependence and were chosen so that the sample was most nearly obeying Ohm's law both in the flux closed and partially saturated state.

### THEORY OF ELECTRON-MAGNON SCATTERING

Detailed calculations of the temperature-dependent resistivity due to electron magnon scattering have been made by Turov<sup>1-3</sup> using a treatment developed by Vonsovski.<sup>4</sup> Vonsovski<sup>4</sup> used a Hamiltonian for the

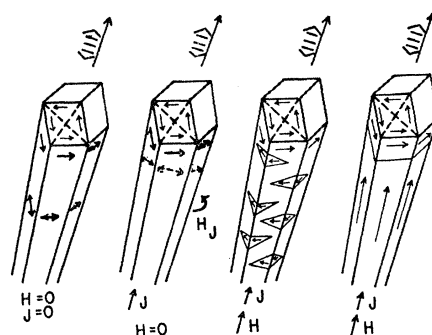


FIG. 7. Possible sequence of domain configurations developing in  $\langle 111 \rangle$  axial whisker with application of longitudinal current and magnetic field.

TABLE I. 4.2°K sample characterization data.

| Sample        | 10°R(294°)<br>(ohm) | RRR <sub>FC</sub><br>R(294°)/R(4.2°) <sub>FC</sub> | RRR <sub>PS</sub><br>R(294°)/R(4.2°) <sub>PS</sub> | R <sub>FC</sub> -R <sub>PS</sub> /R <sub>FC</sub><br>100% | Current<br>(A) |
|---------------|---------------------|--|--|---|----------------|
| Fe<111>RT-1   | 2.29                | 238  | 1560   | 84.7  | 9.5            |
| Fe<111>RT-2   | 1.13                | 137  | 2140   | 93.7  | 8.2            |
| Fe<111>RT-4   | 1.80                | 202  | 601  | 66.3  | 3              |
| Fe<111>No. 30 | 1.071               | 255  | 818  | 68.8  | 3              |
| Fe<110>RT-3   | 4.00                | 169  | 2090   | 91.9  | 3              |
| Fe<100>RT-5   | 10.38               | 131  | 2040   | 93.6  | 3              |
| Fe<100>No. 11 | 1.20                | 145  | 916  | 83.5  | 3              |

system of interacting outer and inner electrons of the form

$$H = H_0 + H_{da} + H_{sd}. \quad (1)$$

The term  $H_0$  represents to a first approximation, the energy spectrum of the system in the form of the sum of energies of the ferromagnons (Bose branch) and conduction electrons (Fermi branch). The second term  $H_{da}$  describes the process of creation and annihilation of ferromagnons due to mutual collisions. The last term includes collision processes between the ferromagnons and conduction electrons. Terms describing the absorption and emission of ferromagnons by conduction electrons are given as follows:

$$\begin{aligned}
 H_{sd} = & \sum_{(\mathbf{k}, \mathbf{q})} C_{\pm}^{(0)}(\mathbf{k}, \mathbf{q}) b_{\mathbf{q}}^* a_{\mathbf{k}-\mathbf{q}}^* \left(-\frac{1}{2}\right) a_{\mathbf{k}} \left(\frac{1}{2}\right) & \Delta m = 0 \\
 & + \sum_{(\mathbf{k}, \mathbf{q})} C_{\pm}^{(0)}(\mathbf{k}, \mathbf{q}) b_{\mathbf{q}} a_{\mathbf{k}+\mathbf{q}}^* \left(\frac{1}{2}\right) a_{\mathbf{k}} \left(-\frac{1}{2}\right) \\
 & + \sum_{(\mathbf{k}\sigma, \mathbf{q})} C_{\pm}^{(1)}(\mathbf{k}\sigma, \mathbf{q}) b_{\mathbf{q}}^* a_{\mathbf{k}-\mathbf{q}}^*(\sigma) a_{\mathbf{k}}(\sigma) & \Delta m = \pm 1 \\
 & + \sum_{(\mathbf{k}\sigma, \mathbf{q})} C_{\pm}^{(1)}(\mathbf{k}\sigma, \mathbf{q}) b_{\mathbf{q}} a_{\mathbf{k}+\mathbf{q}}^*(\sigma) a_{\mathbf{k}}(\sigma) \\
 & + \sum_{(\mathbf{k}, \mathbf{q})} C_{\pm}^{(2)}(\mathbf{k}, \mathbf{q}) b_{\mathbf{q}}^* a_{\mathbf{k}-\mathbf{q}}^* \left(\frac{1}{2}\right) a_{\mathbf{k}} \left(-\frac{1}{2}\right) & \Delta m = \pm 2 \\
 & + \sum_{(\mathbf{k}, \mathbf{q})} C_{\pm}^{(2)}(\mathbf{k}, \mathbf{q}) b_{\mathbf{q}} a_{\mathbf{k}+\mathbf{q}}^* \left(-\frac{1}{2}\right) a_{\mathbf{k}} \left(\frac{1}{2}\right). & (2)
 \end{aligned}$$

The terms are grouped according to the change  $\Delta m$  in the total magnetic quantum number of the system.  $b_{\mathbf{q}}^*$  and  $b_{\mathbf{q}}$  are creation and annihilation operators for magnons of wave vector  $\mathbf{q}$ .  $a_{\mathbf{k}}^*$  and  $a_{\mathbf{k}}$  are creation and annihilation operators for electrons of wave vector  $\mathbf{k}$ . The first two terms corresponding to  $\Delta m = 0$  represent creation or annihilation of a magnon with wave vector  $\mathbf{q}$  accompanied by the creation of an electron in a momentum state  $(\mathbf{k}-\mathbf{q})$  or  $(\mathbf{k}+\mathbf{q})$  and involving the appropriate spin flip of the electron. The additional single-magnon processes for  $\Delta m = \pm 1$  and  $\Delta m = \pm 2$  can be identified in a similar fashion. Higher-order processes involving two or more magnons are neglected.  $C_{\pm}^{(0)}(\mathbf{k}, \mathbf{q})$ ,  $C_{\pm}^{(1)}(\mathbf{k}\sigma, \mathbf{q})$  and  $C_{\pm}^{(2)}(\mathbf{k}, \mathbf{q})$  are the collision probability amplitudes and are determined by the form of the potential energy operator used in the Hamiltonian. Vonsovski<sup>4</sup> has considered two forms of

the interaction operator to be used in the potential energy, one corresponding to the spin-spin interaction between electrons and the other to the spin-orbit interaction due to the interaction of the spin moments of the  $d$ -electrons with the magnetic field created by the moving conduction electron.

In the case of the spin-spin interaction the operator is of the form

$$\begin{aligned}
 \hat{\Phi}(jj') = & V(r_{jj'}) + 4(e\hbar/2mc)^2 \\
 & \times [r_{jj'}^2 (\hat{S}_j \hat{S}_{j'}) - 3(r_{jj'} \hat{S}_j)(r_{jj'} \hat{S}_{j'})] r_{jj'}^{-5}. \quad (3)
 \end{aligned}$$

The spin-spin interaction includes the  $s$ - $d$  exchange interaction and the direct dipole-dipole interaction between spins.  $r_{jj'} = |\mathbf{r}_j - \mathbf{r}_{j'}|$  and refers to the distance between the two interacting electrons and  $\hat{S}_j$  is the spin-vector operator in units of  $\hbar$ .

Vonsovski assumes that the magnetic moment of the  $d$  electron is bound to the lattice site and considers a temperature range  $T > (0.1-1.0^\circ\text{K})$  and  $T \ll T_c$  where  $T_c$  is the Curie temperature. Neglecting magnetic anisotropy effects the magnetic interaction between electrons is viewed as producing a certain average internal field  $4\pi M_s$  superposed on the external field. Using nearest-neighbor approximations for some of the electrostatic exchange type integrals, and using the effective-mass approximation he is able to obtain expressions for the collision probabilities  $C_{\pm}^{(0)}(\mathbf{k}, \mathbf{q})$ ,  $C_{\pm}^{(1)}(\mathbf{k}\sigma, \mathbf{q})$ , and  $C_{\pm}^{(2)}(\mathbf{k}, \mathbf{q})$  due to the spin-exchange interaction. The spin-orbit interaction operator is of the form

$$\hat{\Phi}_{s-0}(jj') = -i4(e\hbar/2mc)^2 r_{jj'}^{-3} [\mathbf{r}_{jj'} \times \nabla_{j'}] \hat{S}_{j'}, \quad (4)$$

where the  $j'$  index refers to the  $d$  electron. This interaction operator leads only to collision processes of the  $\Delta m = \pm 1$  type due to the linearity of the operator relative to  $\hat{S}_{j'}$ . Vonsovski<sup>4</sup> obtains also in this case an expression for the collision operator  $C_{\pm}^{(1)}(\mathbf{k}, \mathbf{q})$ .

Turov<sup>1-3</sup> has used Vonsovski's results to obtain explicit expressions for the temperature dependent resistivity in ferromagnets due to electron-magnon scattering. In the case of the  $s$ - $d$  exchange interaction the resistivity expression obtained in Ref. 1 is given by

$$\rho_T = C_1 [T_0 \ln(2T/T_0)] T - \frac{1}{2} C_2 T_0 T + \frac{1}{8} \pi^2 C_2 T^2. \quad (5)$$

$C_1$  and  $C_2$  are constants depending on the form of the dispersion relation for the electrons and  $T_0$  is a constant on the order of 1°K. For a quadratic dispersion law or for most usual cases  $C_1 \leq C_2$ . Therefore at temperatures  $T > T_0$  the  $s$ - $d$  exchange interaction will provide mainly a quadratic dependence of  $\rho(T)$  on  $T$  which arises from the  $\Delta m = 0$  processes

$$\rho(T) \propto \beta T^2 \quad (s\text{-}d \text{ exchange; } \Delta m = 0). \quad (6)$$

A quadratic dependence on temperature due to the  $s$ - $d$  exchange interaction has also been derived by Kasuya<sup>16</sup> and by Goodings.<sup>17</sup>

In the case of the spin-orbit interaction Turov in Ref. 3 obtains the following expression for the resistivity in the temperature interval  $W_0/k \ll T \ll T_c$ :

$$\rho(T) \approx CW_0^2(T/T_c) \ln(kT/W_0), \quad (7)$$

where  $W_0 = g\mu(H_a + 4\pi M_s) = kT_0$ , and  $(W_0/k)$  is estimated to be on the order of 0.1 to 1°K.

For  $T > (W_0/k)$  the temperature-dependent resistivity due to the spin-orbit interaction is therefore proportional to  $T$ .

$$\rho(T) \propto \alpha T \quad (\text{spin-orbit; } \Delta m = \pm 1). \quad (8)$$

Turov estimates that this will be the main source of any experimentally observed linear dependence in the low-temperature range.

## EXPERIMENTAL RESULTS

### 1°–4.2°K

The temperature dependence of resistance was determined for seven specimens by measuring the resistance at intervals of approximately 0.2°K in the range 1 to 4.2°K. The temperature was determined by standard techniques using measurements of the helium vapor pressure over the bath and carbon resistance thermometry. Calibration of both methods and detailed comparisons of the temperature curves indicated a maximum uncertainty of 20 millidegrees in the temperature measurement. The resistance of the specimen was determined using standard potentiometric methods.

Great care was taken to control the specific domain state of the specimen during the course of each run. In making the measurements with the specimen in the flux closed state (FC) it was found best to attain the maximum resistance by first cycling the applied magnetic field and then to remain at the peak resistance state during the entire run. The peak resistance state was maintained for each measurement by application of a very small increment of slow AC field sweep which allowed us to obtain the exact value of peak resistance at each temperature. Any random cycling to appreciable magnetic fields during the run would produce considerable scatter in the data.

The data for the partially saturated state (PS) were obtained by leaving the applied magnetic field at a single constant value during the course of the entire run. Cycling of the field or changing the measuring current during the run again produced considerable scatter in the data. A set of Helmholtz coils was used to cancel the earth's magnetic field, but this was generally observed to have only a very small effect.

By following the above procedures we were able to obtain smooth curves for all of the specimens measured. Representative curves are shown for samples RT-3 RT-4 and RT-5 in Figs. 8(a), (b), and (c).

Within the accuracy of the experiment the curves indicate a linear dependence of resistance on the temperature. The solid lines in the figures are drawn according to a standard least-squares fit of the data to a straight line. The error bars on the points indicate the mean square deviation computed from the least-squares analysis or the experimental uncertainty, whichever is larger for the given experiment.

The linear coefficient has been obtained by fitting the data to an expression of the form,

$$R(T)/R(294^\circ\text{K}) = R_0/R(294^\circ\text{K}) + \alpha T. \quad (9)$$

Values of the coefficient  $\alpha$  and  $R(0^\circ\text{K})/R(294^\circ\text{K})$  for the seven specimens measured in the present experiments are listed in Table II, along with the average values of  $\alpha$  obtained for both the FC and PS states.

## DISCUSSION OF EXPERIMENTAL RESULTS

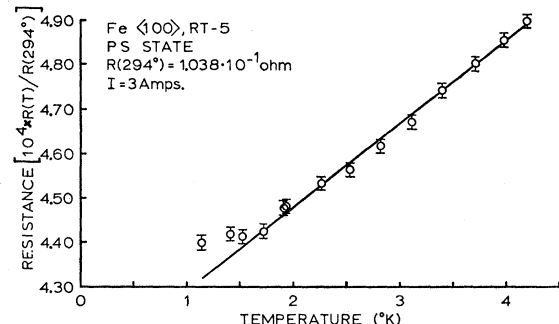
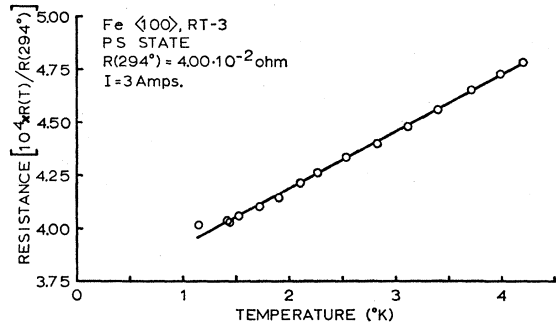
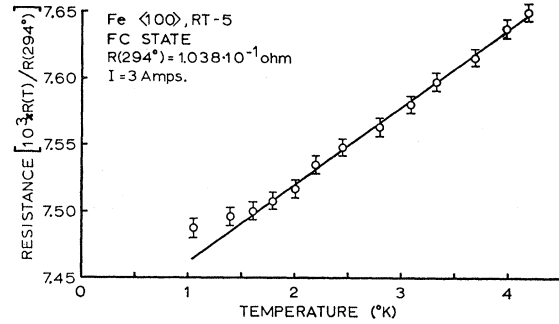
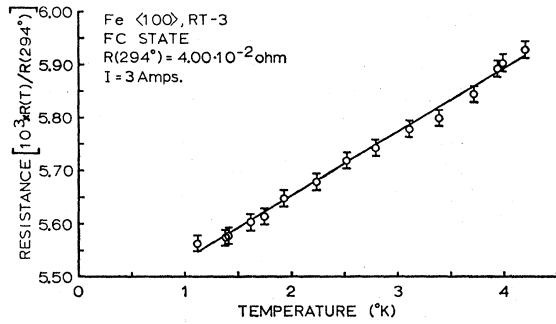
### 1°–4.2°K

Our experimental results indicate that a linear temperature dependence is the dominant behavior for the resistivity of iron in the range 1 to 4.2°K. This linear dependence is most likely that due to electron-magnon scattering and described by the spin-orbit interaction term calculated by Turov.<sup>3</sup> The average linear coefficient for the single domain (partially saturated state) obtained by us is  $2.2 \times 10^{-5} \text{ deg}^{-1}$  or in units of resistivity ( $2.14 \times 10^{-4} \mu\Omega \text{ cm}/^\circ\text{K}$ ). This is to be compared with the latest value of  $1.9 \times 10^{-6} \text{ deg}^{-1}$  obtained by Semenenko and Sudovtsov<sup>6</sup> in the same temperature range and in a magnetic field of 850 Oe. In the flux closed multidomain state (demagnetized state) we obtain an average linear coefficient of  $8.4 \times 10^{-5} \text{ deg}^{-1}$  or in units of resistivity ( $8.2 \times 10^{-4} \mu\Omega \text{ cm}/^\circ\text{K}$ ). The comparable coefficient found by Semenenko and Sudovtsov is  $3.1 \times 10^{-6} \text{ deg}^{-1}$ . In both cases our coefficient is an order of magnitude larger than those measured by Semenenko and Sudovtsov.

The increase in the coefficient is possibly associated with the substantially higher purity and perfection of our samples. Table III lists all of the data of Semenenko and Sudovtsov for iron, nickel and cobalt along with measured resistivity ratios. The difference between RRR ( $H=0$ ) and RRR ( $H \approx 1 \text{ KOe}$ ) is ap-

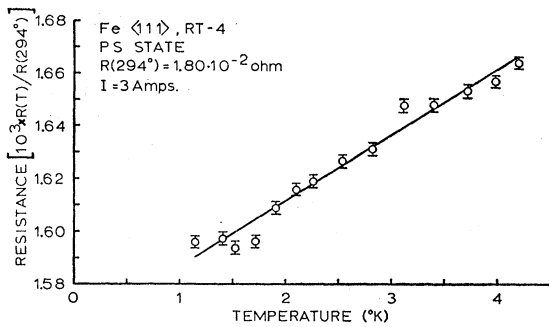
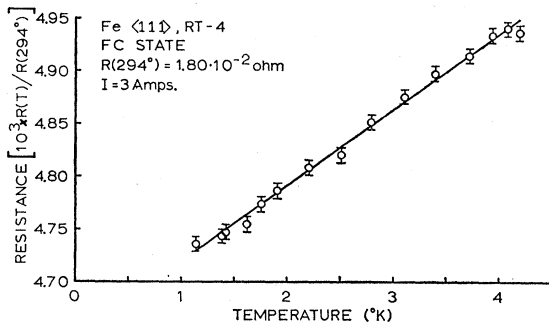
<sup>16</sup> T. Kasuya, Progr. Theoret. Phys. (Kyoto) **22**, 227 (1959).

<sup>17</sup> D. A. Goodings, Phys. Rev. **132**, 542 (1963).



(a)

(c)



(b)

FIG. 8. (a) Temperature dependence of resistance observed in the 1.1 to 4.2°K range for specimen RT-3; (b) Temperature dependence of resistance observed in the 1.1 to 4.2°K range for specimen RT-4; (c) temperature dependence of resistance observed in the 1.1 to 4.2°K range for specimen RT-5.

parently directly related to the mean free path and is therefore some measure of the specimen purity. Non-magnetic impurities in the ferromagnetic matrix might possibly reduce the effective coupling between spin waves and conduction electrons. The present results, as

well as those of Semenenko and Sudovtsov are, however, orders of magnitude larger than the theoretical estimate of  $10^{-9} \text{ deg}^{-1}$  made by Turov in Ref. 2. Ky<sup>18</sup> has re-

<sup>18</sup> Vu Dinh Ky, Zh. Eksperim. i Teor. Fiz. 51, 1476 (1966) [English transl.: Soviet Phys.—JETP 24, 995 (1967)].

TABLE II. The temperature dependence of resistance of iron from 4.2° to 1°K.

| Sample                     | Flux-closure state             |   | Partially saturated state      |   | Current (A) |
|----------------------------|--------------------------------|---|--------------------------------|---|-------------|
|                            | $10^3 R(0^\circ)/R(294^\circ)$ | $10^5 \Delta R(T)/R(294^\circ)\Delta T$ | $10^4 R(0^\circ)/R(294^\circ)$ | $10^5 \Delta R(T)/R(294^\circ)\Delta T$ |             |
| Fe(111)RT-1                | 3.6546±0.0014                  | 8.485±0.417                             | ...                            | ...                                     | 9.5         |
| Fe(111)RT-2                | ...                            | ...                                     | 4.6751±0.0114                  | 1.753±0.035                             | 8.2         |
| Fe(111)RT-4                | 4.6468±0.0028                  | 7.179±0.099                             | 15.618±0.026                   | 2.481±0.302                             | 3           |
| Fe(111) No. 30             | 4.0999±0.0114                  | 9.424±0.330                             | ...                            | ...                                     | 3           |
| Average <111> coefficients |                                | $8.36 \times 10^{-5} \text{ deg}^{-1}$  |                                | $2.12 \times 10^{-5} \text{ deg}^{-1}$  |             |
| Fe(100)RT-3                | 5.4114±0.0158                  | 12.016±0.006                            | 3.6478±0.0050                  | 2.697±0.020                             | 3           |
| Fe(100)RT-5                | 7.4036±0.0021                  | 5.791±0.072                             | 4.1048±0.0026                  | 1.871±0.028                             | 3           |
| Fe(100) No. 11             | 6.5897±0.0030                  | 7.527±0.106                             | ...                            | ...                                     | 3           |
| Average <100> coefficients |                                | $8.44 \times 10^{-5} \text{ deg}^{-1}$  |                                | $2.28 \times 10^{-5} \text{ deg}^{-1}$  |             |

cently examined the theory of resistance anisotropy in ferromagnetic metals due to spin-orbit coupling and has suggested a correction to the theoretical estimate which would bring it into closer agreement with experiment.

Semenenko and Sudovtsov<sup>5,6</sup> also obtained a term proportional to  $T^2$  in the range 1 to 4.2°K for all of their ferromagnetic samples. For iron the most recent value is  $1.65 \times 10^{-6} \text{ deg}^{-2}$ . Within our experimental accuracy we are able to detect no  $T^2$  term. We have calculated the maximum  $T^2$  term allowed within our accuracy and find that it would be on the order of  $10^{-7} \text{ deg}^{-2}$ .

It should be noted, however, that in our samples an apparent  $T^2$  behavior begins to appear if we do not follow the careful procedure required to maintain the same magnetic state at each temperature. For example, data obtained on RT-1 is shown in Fig. 9. Both the flux closed and partially saturated states show substantial  $T^2$  behavior. A cycling of the magnetic field has been carried out before each measurement. We feel that the domain structure is slightly different

after each cycling, particularly as the temperature is successively lowered with a corresponding increase in coercive force. Since the resistance is such a sensitive function of domain structure we feel this slight variation in domain structure may be introducing a temperature dependence which is not a true spin wave scattering term.

The curves of Fig. 9 were fitted by an expression  $R(T)/R(294^\circ\text{K}) = \gamma + \alpha T + \beta T^2$ . The  $T^2$  coefficients were  $1.6 \times 10^{-5} \text{ deg}^{-2}$  and  $2.5 \times 10^{-6} \text{ deg}^{-2}$  in the flux closed and partially saturated states, respectively. The order of magnitude decrease observed for the partially saturated state is somewhat indicative that the  $T^2$  term dies out as the domains are removed. The flux closed state also showed a linear coefficient of  $4.90 \times 10^{-5} \text{ deg}^{-1}$  as compared to the  $8.4 \times 10^{-5}$  obtained for RT-1 in the purely linear experiment. (Table II). This is a rather small change and one concludes that the  $T^2$  term has simply been added to the temperature dependence, at least in first approximation.

The large increase of the linear coefficient in the flux closed versus saturated state is not understood at

TABLE III. Data of Semenenko and Sudovtsov and present data.  $R(T)/R(0^\circ\text{C}) = R(0^\circ\text{K})/R(0^\circ\text{C}) + \alpha T + \beta T^2$ .

| Ref.                             | Metal  | H (Oe) | $\alpha$ (deg <sup>-1</sup> ) | $\beta$ (deg <sup>-2</sup> ) | $R(0^\circ\text{C})/R(0^\circ\text{K})$                       |
|----------------------------------|--------|--------|-------------------------------|------------------------------|---|
| a, b (1962)                      | Iron   | 0      | $3.1 \times 10^{-6}$          | $1.10 \times 10^{-6}$        | 253   |
| a, b (1962)                      | Iron   | 850    | $1.9 \times 10^{-6}$          | $1.65 \times 10^{-6}$        | 385   |
| c (1956)                         | Iron   | 0      | $(4-4.9) \times 10^{-6}$      | $(1-1.2) \times 10^{-6}$     | 25  |
| c (1956)                         | Nickel | 0      | $(0.8-22) \times 10^{-6}$     | $2.7 \times 10^{-6}$         | 100   |
| Average values from present exp. | Iron   | 0      | $8.4 \times 10^{-5}$          | $\beta < 10^{-7}$            | (182) <sub>Av</sub>   |
|                                  | Iron   | 1200   | $2.2 \times 10^{-5}$          | $\beta < 10^{-7}$            | $(1452)_{Av} \cdot R(294^\circ\text{K})/R(4.2^\circ\text{K})$ |
| d (1964)                         | Cobalt | 0      | $(3.3-5.5) \times 10^{-6}$    | $(1.5-1.7) \times 10^{-6}$   | 26  |

<sup>a</sup> See Ref. 5.

<sup>b</sup> See Ref. 6.

<sup>c</sup> E. E. Semenenko, A. I. Sudovtsov, and A. D. Shvets, Zh. Eksperim. i Teor. Fiz. 42, 1488 (1962) [English transl.: Soviet Phys.—JETP 15, 1033 (1962)].

<sup>d</sup> E. E. Semenenko, A. I. Sudovtsov, and N. V. Volkenshtein, Zh. Eksperim. i Teor. Fiz. 45, 1387 (1963) [English transl.: Soviet Phys.—JETP 18, 957 (1964)].



present. The factor of 3.8 is observed for both the  $\langle 100 \rangle$  and  $\langle 111 \rangle$  specimens and appears rather consistently from one specimen to another. One possibility is that the spin-wave density or spectrum is substantially different near and within domain walls than it is in the volume of a single domain. Such a possibility exists since the spin rotation in a domain wall will tend to destroy the energy gap which is normally present in the spin-wave dispersion curve due to the average internal field of  $4\pi M_s$ . A second possible effect could enter via the dependence of the spin-orbit scattering probability on the relative orientation of  $\mathbf{M}_s$  and  $\mathbf{J}$ . Any strong dependence would, of course, modify the multidomain behavior versus the single domain behavior. However, theoretical considerations of the anisotropy in the spin-orbit scattering probability indicate that the scattering probability is highest for  $\mathbf{M}_s \parallel \mathbf{J}$ . This effect would therefore reduce the scattering in the multidomain state. This argument has, in fact, been used by Smit<sup>19</sup> and by Marsocci<sup>20</sup> to explain the positive longitudinal magnetoresistance observed at room temperature in ferromagnetic metals.

In analyzing the data, we have so far used only a single coefficient obtained from the best fit to the experimental curves. This is also the standard procedure which has been used in previous treatments of experimental data on the temperature dependence of resist-

ance. However, in ferromagnetic metals a complete analysis should separate the temperature-dependent resistivity into two parts, one due to the direct electron-magnon scattering and a second indirect term due to the dependence of the magnetoresistance on relaxation time. In the above experiments the appropriate magnetoresistance is that due mainly to the internal magnetic field of  $4\pi M_s \approx 22$  kOe, assuming that this is the value of  $B$  seen by the conduction electron within each domain when the external field is small ( $H_a \ll 4\pi M_s$ ).

In a field of 22 kOe and for a mean free path which we estimate to be  $>10\mu$  the magnetoresistance would be in transition from the low-field region ( $\omega_c\tau \ll 1$ ) to the high-field region ( $\omega_c\tau \gg 1$ ). In both regions the transverse magnetoresistance is in theory proportional to  $(\omega_c\tau)^2$  while in the low-field region the longitudinal magnetoresistance is proportional to  $(\omega_c\tau)^2$  and saturates in high fields (see Blatt<sup>21</sup> or Fawcett<sup>22</sup> for detailed discussion). For applied fields from 20 to 50 kOe we actually observe a dependence described by  $(\omega_c\tau)^n$  where  $1 < n < 2$  for both cases with  $n_l < n_t$ . The exact value of  $n$  to be used in calculating the temperature-dependent magnetoresistance term with  $H_a \ll 4\pi M_s$  is not completely certain, but the total  $\tau$ -dependent resistivity would be of the form

$$\rho(\tau) = C_1(1/\tau) + C_2(\omega_c\tau)^n$$

or

$$\rho(\tau) = C_1(1/\tau) + C_2[(eH_a + 4\pi M_s e)/2mc\tau]^n, \quad (10)$$

where the demagnetizing factor has been neglected in the second expression. The first term is the direct linear spin-wave scattering term due to spin-orbit interaction and is decreasing with decreasing temperature (increasing  $\tau$ ). The second term is the magnetoresistance contribution which is increasing for decreasing temperature (increasing  $\tau$ ). Separation of these two terms will require considerably more experiment and analysis, but several general points can be made. Above some critical applied field the second term will become dominant and the observed temperature dependence of resistance should reverse sign. Even in low-applied fields the second term is probably large enough in high-purity specimens that the measured linear coefficient is smaller than the true spin-wave scattering coefficient. The importance of the second term is clearly proportional to the purity of the sample, and introduces an added complication in measuring the true spin-wave scattering in high-purity specimens.

The second term, however, does not account for the factor of 3.8 observed between the flux closed and partially saturated coefficients since  $H_{PS} \ll 4\pi M_s$  and  $n_l < n_t$ . If anything, the actual spin-wave scattering

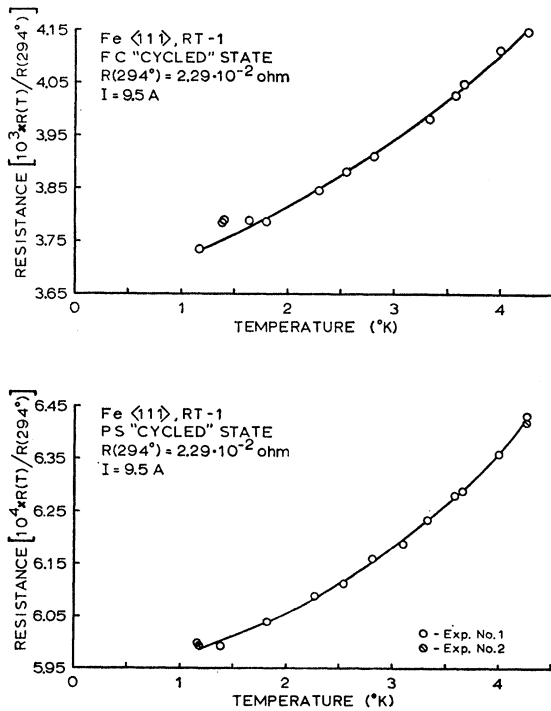


FIG. 9. Temperature dependence of resistance obtained in the 1.1 to 4.2°K range when the specimen is magnetically cycled at each temperature.

<sup>19</sup> J. Smit, *Physica* 16, 612 (1951).

<sup>20</sup> Velio A. Marsocci, *Phys. Rev.* 137, A1842 (1965).

<sup>21</sup> Frank J. Blatt, in *Solid State Physics*, edited by F. Seitz and D. Turnbull (Academic Press Inc., New York, 1957), Vol. 4, p. 199.

<sup>22</sup> E. Fawcett, *Advan. Phys.* 13, 139 (1964).

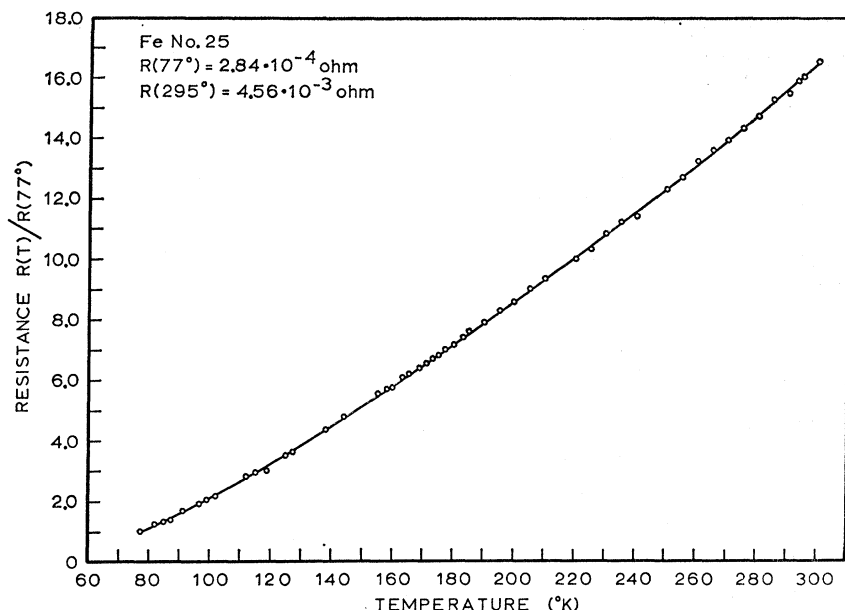


FIG. 10. Temperature dependence of resistance measured in the range 78 to 300°K.

coefficient when corrected for the second term would show a greater ratio  $\alpha_{FC}/\alpha_{PS}$  than 3.8.

For fields  $H_a > 4\pi M_s$ , a strong decrease in the coefficient with increasing field should begin to show up because of the second term. In addition, the spin-wave scattering itself should be reduced by applied fields,  $H_a$ , on the order of  $4\pi M_s$ . This can be argued simply on the basis of a reduction in the spin-wave density by the applied field due to an increase in the energy gap appearing in the dispersion relation for the magnon energy.

$$\epsilon_q = J(aq)^2 + g\mu(H_a + 4\pi M_s) = J(aq)^2 + W_0,$$

$J = d-d$  exchange integral,

$a =$  lattice constant,

$q =$  magnon-wave vector.

$W_0$  enters the resistivity expression as previously given in formula (7) above.

#### TEMPERATURE DEPENDENCE IN THE RANGE

##### 4.2° to 295°K

For the temperature range extending from 4.2°K to room temperature most experiments on iron have indicated a temperature dependence of the form  $\rho = \beta T^n$  where  $n$  has ranged from 2 to 5 depending on the sample and specific temperature interval. Measurements have been made by White and Woods<sup>23</sup> for all three ferromagnetic metals Fe, Co, and Ni in the range from helium temperatures to room temperature. For

<sup>23</sup> G. K. White and S. B. Woods, Phil. Trans. Roy. Soc. (London) **A251**, 273 (1958).

temperatures below 10°K they find a dependence of the form  $\rho = \beta T^2$  with  $\beta = 0.13 \times 10^{-4}$  ( $\mu\Omega \text{ cm deg}^{-2}$ ). For temperatures 20°K to approximately 100°K they find a dependence of the form  $\rho = \alpha T^{3.3}$ , while for temperatures from 100 to 295°K their data indicate nearly a linear dependence of resistance on temperature. Kondorskii *et al.*,<sup>24</sup> have made measurements on iron and nickel, as well as on nickel-copper alloys in the range 4.2 to 78°K. Below about 30°K they find a predominantly  $T^2$  behavior for iron with the coefficient  $\beta = 0.4 \times 10^{-4}$  ( $\mu\Omega \text{ deg}^{-2}$ ), about three times larger than that found by

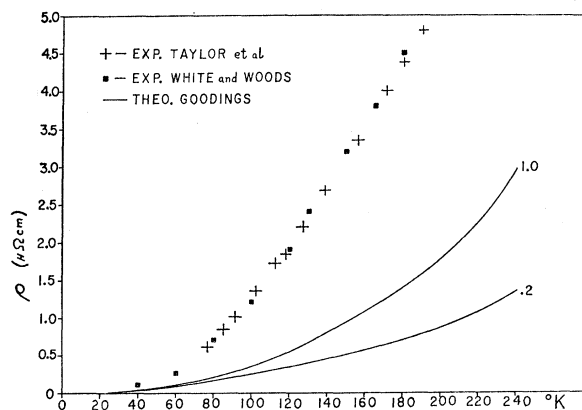


FIG. 11. Theoretical curves for the temperature-dependent magnetic resistance calculated by Goodlings (Ref. 17), solid lines. Experimentally measured values are shown by points; ■, data of White and Woods; (Ref. 22) +, data from present experiments. Theoretical curves are shown for two values of  $|\mathbf{k}_{F1} - \mathbf{k}_{F2}|$ .

<sup>24</sup> E. I. Kondorskii, O. S. Galkina, and L. A. Chernikova, Zh. Eksperim. i Teor. Fiz. **34**, 1070 (1958) [English transl.: Soviet Phys.—JETP **7**, 741 (1958)].

White and Woods. Kondorskii *et al.*<sup>24</sup> have also analyzed their data for other dependences such as  $T^{3/2}$  and  $T^5$ . The appropriate coefficients can be found in the original paper. They find that for  $T > 30^\circ\text{K}$  a  $T^5$  term begins to play an essential role. Such a term mixed with a  $T^2$  term could, of course, account for White and Woods observation of  $\rho \sim T^{3.3}$  for temperatures above  $20^\circ\text{K}$ .

We have made preliminary measurements on our iron specimens in the range 78 to  $295^\circ\text{K}$  and data for specimen #25 are shown in Fig. 10. In the range  $78\text{--}100^\circ\text{K}$ , the best fit of the data to a single power law is  $\rho = \beta T^{2.8}$  while from  $100\text{--}295^\circ\text{K}$  the best fit to a single power law is  $\rho = \beta T^{1.7}$ . The magnitude of our resistivity is in essential agreement with the measurements of White and Woods and comparison is made in Fig. 11 along with theoretical curves for the magnetic resistance calculated by Goodings.<sup>17</sup>

For temperatures above  $4.2^\circ\text{K}$  one generally expects the resistivity of ferromagnetic metals to show a dependence on higher powers of the temperature, ( $T^2$  or greater). This will be connected with either the  $s$ - $s$  scattering due to spin-exchange interaction and given by formula (6) above or to  $s$ - $d$  interband transitions which become important above some critical temperature.

Goodings<sup>17</sup> has made the most complete calculation of the resistivity contribution due to  $s$ - $d$  interband transitions. He finds that for temperatures above approximately  $20^\circ\text{K}$  the scattering of  $s$  electrons into holes in the  $d$ -band is the main source of resistance, being an order of magnitude larger than the single-band scattering. Goodings uses a two-band model to treat the conduction electrons and the itinerant  $d$  electrons, the two sheets of the Fermi surface being separated by some radial distance  $|\mathbf{k}_{F1} - \mathbf{k}_{F2}|$ . As a consequence of momentum conservation, the wave vector of the spin wave associated with the interband transition must be greater than the radial distance between the two Fermi surfaces ( $|\mathbf{k}_{F1} - \mathbf{k}_{F2}| \leq q \leq \mathbf{k}_{F1} + \mathbf{k}_{F2}$ ). The interband transitions therefore become important at temperatures high enough to excite spin waves of wave vector greater than this critical value. Using this model plus a number of other simplifying assumptions Goodings obtains the theoretical curves shown in Fig. 11. The curves represent only the "spin-disorder" scattering and are consequently lower than the experimental curves since at higher temperatures the  $s$ - $d$  scattering due to lattice vibrations is also an important contribution.

Further measurements of the temperature dependence of resistivity in the present iron whisker specimens for the range  $4.2\text{--}294^\circ\text{K}$  are in progress and will be reported later.

### CONCLUSIONS

Measurements of the temperature-dependent resistivity in the 1 to  $4.2^\circ\text{K}$  range indicate that the re-

sistivity of iron varies linearly with temperature. The data have been fitted to an expression of the form

$$R(T)/R(294^\circ\text{K}) = R(0^\circ\text{K})/R(294^\circ\text{K}) + \alpha T,$$

and  $\alpha$  has been determined for seven specimens with  $\langle 100 \rangle$  and  $\langle 111 \rangle$  axial orientations. Values of  $\alpha$  have been obtained for both the flux closed multidomain state and for the partially saturated state attained in an applied longitudinal field of 1000 Oe. The average values obtained for  $\alpha$  are  $8.4 \times 10^{-5}$  and  $2.2 \times 10^{-5} \text{ deg}^{-1}$  for the flux closed and partially saturated states, respectively. These values of the linear coefficient are an order of magnitude larger than reported in any of the previous measurements. We believe that this may be connected with the substantially higher purity of the specimens used in the present experiments. At present we have no explanation for the factor of 3.8 in the coefficient for the flux closed versus partially saturated state.

The linear behavior is in qualitative agreement with the spin-wave scattering theories developed by Vonsovski<sup>4</sup> and Turov.<sup>1-3</sup> These theories predict that the linear dependence will arise from a magnon-electron scattering due to spin-orbit interaction. However, it is difficult to account for the large magnitude of the coefficient  $\alpha$ .

Our results indicate that any  $T^2$  temperature dependence in the 1 to  $4.2^\circ\text{K}$  range is very small with a coefficient of  $10^{-7} \text{ deg}^{-2}$  or less. An apparent  $T^2$  behavior can, however, be introduced by arbitrarily cycling the magnetic field.

In general, we find that measurements on these very high-purity samples require considerable care due to the occurrence of the strong negative magnetoresistance and deviations from Ohm's law. A complete understanding of these effects is not yet available, but they are to a large extent induced by the measuring current.

It is also clear that the ordinary magnetoresistance term due to the average internal magnetic field should be taken into account in analyzing the true spin-wave scattering coefficient. Experiments are presently underway in high-magnetic fields and these should enable us to correct the low-field data by taking into account the magnetoresistance term. Measurements of the temperature coefficient in high-magnetic fields should also give us information on the energy gap in the spin-wave spectrum.

### ACKNOWLEDGMENTS

The authors would like to acknowledge many stimulating discussions with Professor Leo Falicov, Professor Martin Zuckermann, Professor Miguel Kiwi, Professor Vittorio Celli, and Professor N. Cabrera. The authors also acknowledge the valuable services of Phillip Sommer, Warner Frewer, and George Bartsch in construction of the apparatus.